SSRG International Journal of Electrical and Electronics Engineering
ISSN: 2348-8379/ https://doi.org/10.14445/23488379/IJEEE-V13I1P109

Volume 13 Issue 1, 95-102, January 2026

Original Article

Enhancing Ultra-Wideband Breast Imaging: A Low Noise Amplifier with Minimized Group Delay Variation

Nuha A. Rhaffor[1,2], Rohana Sapawi*[1], Sofiyah Sal Hamid[2], Selvakumar Mariappan[2]

[1]*Department of Electrical and Electronics Engineering, Faculty of Engineering, Universiti Malaysia Sarawak, 94300 Kota Samarahan, Sarawak, Malaysia.*
[2]*Collaborative Microelectronic Design Excellence Centre (CEDEC), Universiti Sains Malaysia, 11900 Bayan Lepas, Penang, Malaysia.*

**Corresponding Author : srohana@unimas.my*

Received: 06 November 2025 Revised: 08 December 2025 Accepted: 07 January 2026 Published: 14 January 2026

Abstract *- This research presents a 180 nm CMOS technology ultra-wideband low-noise amplifier with low group delay variation for breast imaging applications. The proposed design employs a hybrid LNA configuration that integrates a cascoded architecture with inductive source degeneration and an inductive peaking structure functioning within the frequency range of 3.1 to 10.6 GHz. The measurement results demonstrate a maximum gain, S_{21}, of 13.6 dB; an input reflection coefficient, S11, of less than –10 dB; and a reverse isolation, S12, of less than –33.5 dB at the measurement stage. It achieves an excellent group delay of 117.6 ±24.8 ps, an input 1-dB compression point of -12 dBm, an input third-order intercept point of 2 dBm, and a minimum noise figure of 5.2 dB. Furthermore, this research identifies three inductors as the dominant factor contributing to low group delay variation through simulation and theoretical analysis.*

Keywords *- Breast cancer, Group delay variation, Low noise amplifier, Microwave breast imaging, UWB.*

1. Introduction

Breast cancer is the primary cause of cancer in women globally. Early detection is critical to improve treatment outcomes, thereby motivating the development of non-invasive and cost-effective imaging systems that are capable of high spatial resolution. Techniques such as ultrasound, X-ray, mammography, and other breast imaging techniques are commonly used in clinical practice for the early diagnosis of breast cancer [1-4]. This method has traditionally been known as an effective method; however, many obstacles are presented, including ionizing radiation exposure, patient discomfort, and the impossibility of detecting small abnormalities. Among the various emerging technologies, Ultra-Wideband (UWB) microwave imaging has received great attention because of its ability to differentiate malignant and healthy tissues based on dielectric contrast, while operating with low power, non-ionizing radiation, and the possibility for portability [1, 5, 6]. Figure 1 displays the UWB microwave imaging for the breast cancer detection system [7]. In this configuration, an array of transceivers, each coupled to an antenna, transmits short UWB pulses into the breast tissue and receives the backscattered signals [8]. These reflections are normally weak, requiring careful amplification. The Low Noise Amplifier (LNA), positioned at the front end of the receiver chain, is responsible for amplifying these signals while maintaining their integrity.

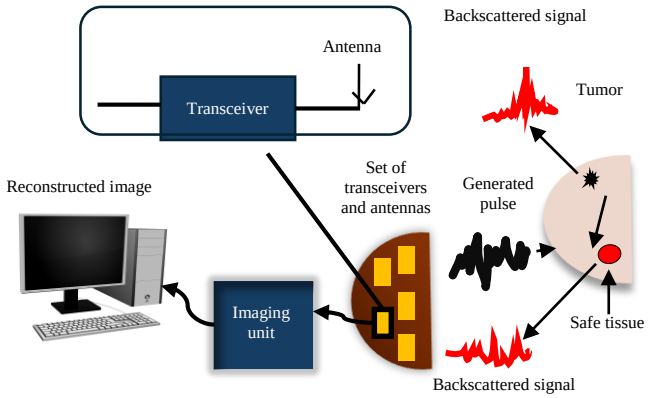

Fig. 1 UWB microwave imaging for breast cancer detection system [7]

A comprehensive review of LNA designs from 1960 to 2019 [9] as well as recent studies until 2025 [10-15] found that the design of UWB LNAs has focused on metrics such as noise figure, gain flatness, linearity, and impedance matching. Most of this work was done for communication and radar systems. In contrast, UWB breast imaging relies on time-domain signal quality to reconstruct the image accurately. In this context, group delay plays a crucial role as it is a frequency derivative of the phase response. Nonlinear group delay causes phase distortion over the frequency band,

resulting in pulse spreading and signal distortion. This directly degrades the image resolution system's ability to accurately localize tumours.

Despite the critical role of timing accuracy, group delay behaviour in LNA design for biomedical imaging has received less attention. While several recent radar-oriented studies have begun to address group delay minimization [16], the findings have not been translated to breast imaging applications. Prior research in [17, 18] has demonstrated the consequences of group delay variation on pulse integrity, highlighting how inconsistent group delay across a UWB band can lead to significant signal distortion.

Specifically, distorted phase relationships between harmonic components can reduce system resolution and impair tumour localization. Studies simulating group delay performance in microwave-based breast imaging systems [19] have shown that maintaining a flat group delay profile across the frequency band significantly reduces distortion, thereby improving detection reliability. A thorough analysis and discussion of group delay in LNA design, particularly for UWB breast imaging systems, remains lacking. This gap in the literature motivates the current research. In contrast to earlier research that used it as a secondary parameter, this study focuses on group delay variation as a primary design target in a UWB LNA for breast imaging.

A hybrid cascoded LNA with inductive source degeneration and inductive peaking is proposed and experimentally validated. In addition, the dominant factors influencing group delay variation in UWB breast imaging systems are identified and analysed. This study advances breast imaging system development by including group delay factors into the design and evaluation process of LNAs for biomedical applications. The rest of the paper is structured as follows. Section 2 of this work focused on circuit implementation with 180 nm RF CMOS technology, while Section 3 went into detail on group delay analysis. The measurement results for the suggested design are compiled in Section 4, and the article concludes in Section 5.

2. Circuit Implementation

Figure 2 illustrates the schematic design of the proposed LNA, which uses CMOS 180 nm technology and operates at frequencies from 3.1 to 10.6 GHz. Table 1 displays the parameters of all components utilized in this design. The proposed schematic consists of a cascoded design and a common source with inductive peaking. Cascoded structure is a conventional topology in LNA design, but an optimized combination of cascoding with other techniques, like inductive source degeneration and gate inductor, can produce wideband, input matching, and low group delay across the frequency range. The choice of a two-stage design provides additional.

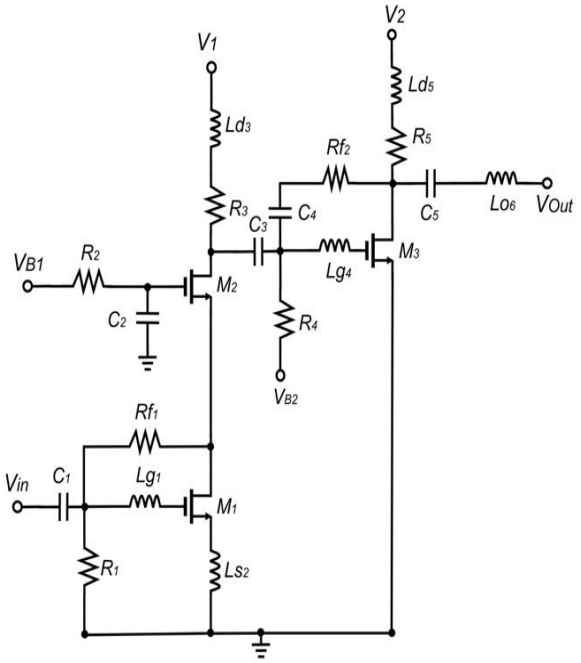

Fig. 2 Schematic design for the proposed UWB LNA.

Table 1. Component parameters

Parameter	Value	Parameter	Value
M_1	200/180nm	Lg_4	1.6nH
M_2	200/180nm	Ld_5	3.1nH
M_3	120/180nm	Lo_6	178pH
C_1	10pF	R_1	50KΩ
C_2	10pF	R_2	1KΩ
C_3	5pF	R_3	116Ω
C_4	200fF	R_4	2KΩ
C_5	1pF	R_5	14Ω
Lg_1	824pH	Rf_1	200Ω
Ls_2	208pH	Rf_2	750Ω
Ld_3	3.5nH		

Gain to further amplify the signal over the entire frequency range. Besides, this design provides high reverse isolation and stability. Good reverse isolation is required to prevent leakage signals from the output back to the input, which might cause instability or oscillation. A single-stage topology is unable to produce high gain across the frequency band, but it does give lower noise when compared to a two-stage topology. A three-stage design is more effective at boosting the gain; however, it produces higher noise and requires more chip area. The increase in noise at each stage is caused by the addition of active components, each of which will add its own noise to the signal. Thus, in this design, a two-stage topology was chosen, as it can produce high gain with minimum noise. The first stage consists of transistor M_1 and

M_2, as well as inductive source degeneration, Ls_2. At the input, capacitor C_1 and resistor R_1 function as a high-pass filter. The high-pass filter prevents low-frequency noise (flicker noise 1/f noise) from entering the LNA, which is prevalent at lower frequencies in CMOS technologies. The R_1 as an input matching network helps to improve and stabilize the input impedance, and it is commonly used in LNA design. However, it contributes to thermal noise; therefore, the trade-off slightly affecting the NF must be tolerated. The peaking inductor, L_{g1}, extends the bandwidth and increases gain at higher frequencies. The feedback resistor Rf_1 controls the drain current. Inductors Lg_1, Ls_2, and Ld_3 play an important role in lowering group delay variation.

The second stage of the proposed LNA uses a common source with an inductive peaking technique. The main amplifying device is the transistor, M_3, which receives a biasing voltage from V_{B2} to set the right operating point. The peaking inductors, Lg_4 and Ld_5, had a similar role in improving bandwidth and increasing high-frequency gain. The resistor, R_5, regulates the drain current and ensures a stable output. The feedback resistor, Rf_2, produces a negative feedback loop by feeding some of the output voltage back into the input. The addition of feedback resistors in the first and second stages of this architecture broadens the input bandwidth, allowing for wideband input matching. It also improves the stability, resulting in a K-factor >1. Besides, it is critical to flatten the gain and group delay across the entire frequency band. However, feedback resistors can introduce thermal noise, which has a direct impact on the overall NF, as each resistor generates thermal noise. Prior to this, the feedback resistor acts as a noise source, which gets worse since it is linked to both the input, causing noise to propagate both forward and backward.

3. Group Delay Analysis

GD is the amount of time delayed by each of the various frequency components of a signal as they move through the amplifier, which is defined as the negative derivative of phase with respect to angular frequency as expressed in Equation 1. In order to reduce signal distortion and maintain the quality of transmitted data, the GD must be low over the frequency range.

$$G_d = -\frac{d\theta}{d\omega} \tag{1}$$

Constant group delay is required in RF applications to ensure that all frequency components of the signal arrive at the output without delay, hence, preserving signal shape. This requirement is more crucial than in conventional communication-oriented LNAs, where phase linearity is frequently used as a secondary performance parameter. The suggested circuit primarily relies on inductors Ls_2, Lg_1 , and Ld_3 to influence group delay behavior. The source degeneration inductor, Ls_2, and the input gate, Lg_1, are critical components for achieving an input impedance near 50 Ω and play a crucial role in achieving flat group delay across the frequency band. When the input matching is properly matched, it ensures minimal reflections, which contribute to a smooth phase response and hence make the GD flat over the frequency band. Inductor Ls_2 also functions as a phase linearizer, stabilizing the phase response and linearizing the input impedance across the entire frequency range. As demonstrated in Equation 1, group delay is measured by how much the phase of the signal changes with respect to frequency; hence, the phase response must be linear to achieve a stable group delay. A nonlinear response in which the pulse arrives at different times will produce a signal distortion.

Another critical component that helps in achieving flat and low group delay is the peaking inductor, Ld_3. Peaking inductors typically serve to extend the bandwidth and flatten the phase response at high frequency, hence flattening the GD over the frequency range. Figure 3 illustrates the effect of inductors on group delay variation. Reducing the inductor's value will result in low group delay variations; however, it has a negative influence on gain performance, impedance matching, and NF. On the other hand, increasing the values of these inductors increases group delay variation. Hence, the parameters of these inductors are carefully optimized, and it is verified through a parametric analysis.

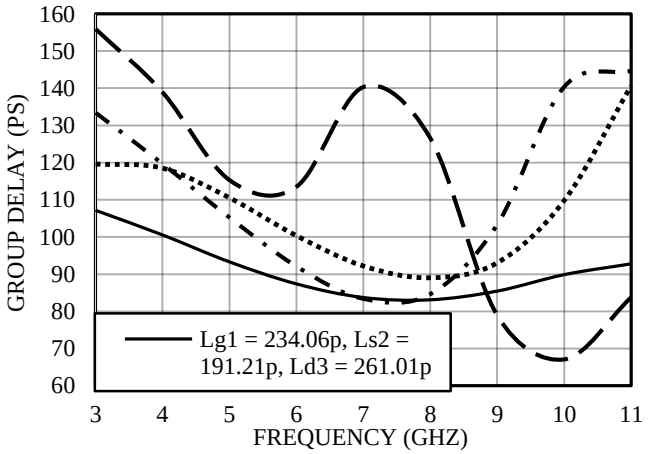

Fig. 3 Effect of inductance on the group delay

The group delay analysis starts by finding the LNA's transfer function H(s). The transfer function will define the relationship between input and output voltages in the frequency domain. The transfer function of the circuit is as in Equation 2, where $s = j\omega$ and $\omega = 2\pi f$.

$$H(s) = \frac{gm_2(R_3+sLd_3||ro_2)(1+gm_1sLs_2)}{g_{m1}(r_{o1}||Rf_1+sLg_1)} * \frac{gm_3(ro_3||R_5+sLd_5+sLo_6)(R_4||sLg_4)+Rf_2}{R_4||sLg_4} \tag{2}$$

The group delay expression for the overall transfer function can be derived as,

$$G_d = [-\frac{ro_2 Ld_3}{\omega^2 Ld_3{}^2 + ro_2{}^2} + \frac{g_{m_1} Ls_2}{1+(gm_1 \omega Ls_2)^2} + \frac{ro_1 Rf_1 Lg_1}{ro_1 + Rf_1} + \omega^2 Lg_1{}^2]$$

$$+[\frac{ro_3 R_5 Ld_5 Lo_6}{ro_3 + R_5} + \omega^2 Ld_5{}^2 - \frac{Lg_4}{1+\omega^2 Lg_4{}^2} + \frac{Lg_4}{1+\omega^2 Lg_4{}^2}] \quad (3)$$

Equation 3 shows that the GD is the sum of a few frequency-dependent elements, where each is dominated by an inductor. Though there are other secondary components like inductors and resistors that appear in the expression, they did not give much influence on the GD variation within the frequency range as their coefficient are too small to influence the GD. The inductors Ls_2, Lg_1, and Ld_3 appear dominantly in the expression. These inductors are placed in the very sensitive part of the signal path, that is, the input gate, source degeneration, and cascode drain of the first stage in the proposed design. Optimizing these inductors will produce changes in the simulated group delay graph, as shown in Figure 3. Each inductor contributes a peak or dip in the group delay. Based on Figure 3, increasing the inductor value will increase the magnitude since the inductor creates a natural resonance, thus increasing the peak and dip in the graph. A high peak and dip make the GD graph become more curved and change more throughout the frequency range. A smaller inductor value maintains a smooth and more uniform graph as it has a weak phase shift due to less energy stored in the inductor, thus this contributes to smaller GD variation.

4. Results and Discussion

The suggested LNA was designed and simulated utilizing 180 nm Silterra Technology. Figure 4 shows the die layout for the proposed LNA. Figure 5 displays the measurement result for the S-parameter. The average measured gain, S_{21}, is 11.2 dB and remains above 10 dB across the frequency range, with the maximum gain achieved being 13.6 dB at 4 GHz. The optimal gain is attained by a two-stage topology with cascoded design architecture. The gain distribution of each stage was optimized at both schematic and layout design.

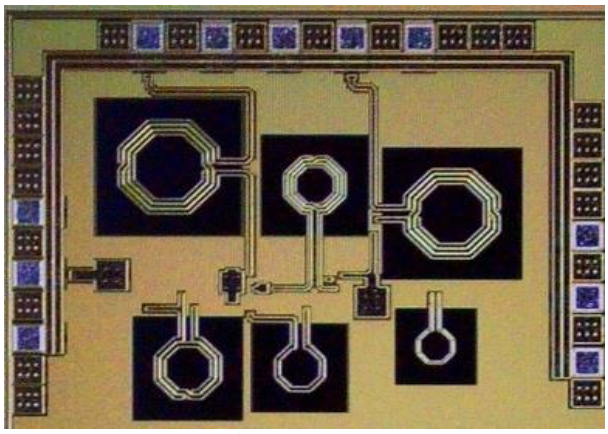

Fig. 4 Die micrograph of the completed LNA (1.288 x 0.965mm)

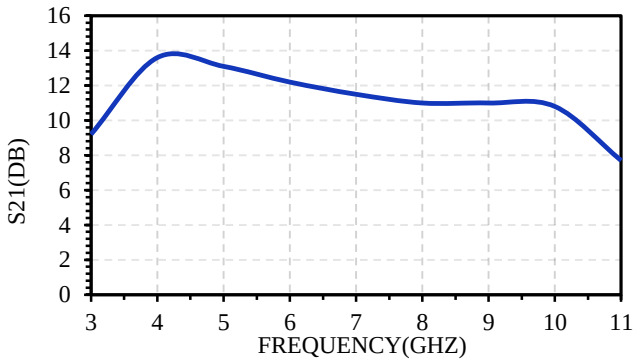

(a)

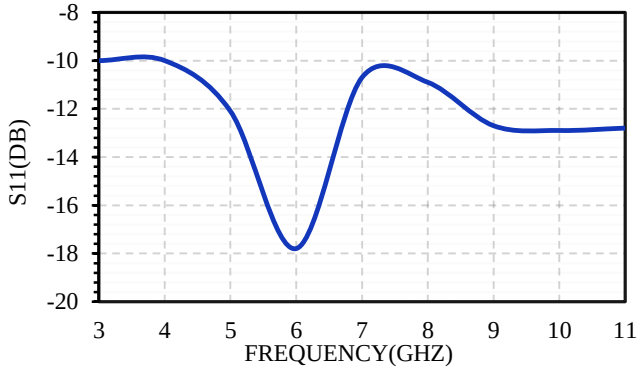

(b)

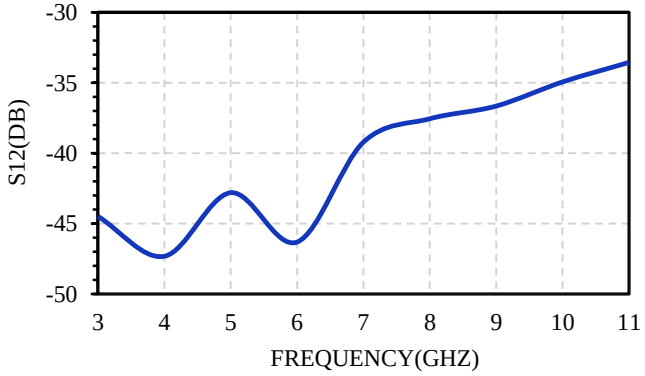

(c)

Fig. 5 Measurement result for S-parameters (a) S_{21}, (b) S_{11}, and (c) S_{12}.

The first stage of the LNA design provides less gain, while the second stage contributes extra gain, controls the gain across the entire frequency range, and determines the overall NF. The proposed LNA achieves the measurement result of less than -10 dB for the input return loss, S_{11}, with a minimum value of -17.8 dB at 6 GHz. The minimum value achieved at 6 GHz indicates good impedance matching, implying maximum power transfer from the antenna to the RF input. The gate inductor, source degeneration inductor, resistor, and feedback resistor work together to provide appropriate impedance matching. When the value of all combined components is precisely tuned, the input impedance Z_{in} equals

the source impedance of 50 Ω. Equation 4 depicts the relationship between all selected components at the input matching stage.

$$Z_{in} = R_1 + j\omega Lg_1 + (\frac{1}{j\omega C_{gs}} || Z_s) \quad (4)$$

Where gm_1Vg is the transconductance, and Z_s is the impedance at the source of M_1.

$$Z_s = j\omega Ls_2 + \frac{gm_1 V_g R f_1}{1+gm_1 R f_1} \quad (5)$$

As for the reverse isolation, S_{12} achieves less than -33.5 dB. Figure 6 shows the group delay variation of the proposed LNA. It achieves a GD variation of ±24.8 ps. The achieved results are due to the influence of the peaking inductor and inductive source degeneration. Proper tuning of the inductors helps in the improvement of the GD result. However, there will be a trade-off in other performance, particularly gain, input matching, and NF; therefore, it is critical to monitor other performances when the GD variation is at a low level. The proposed LNA can achieve low group delay with a stable gain. In breast imaging detection, the received signal's timing is crucial because it must match the original pulse's shape and timing to create an accurate image. Irregular group delay would distort the pulse, making it more difficult to identify or find abnormalities in the image. The achieved GD of ±24.8 ps is excellent for UWB breast imaging applications.

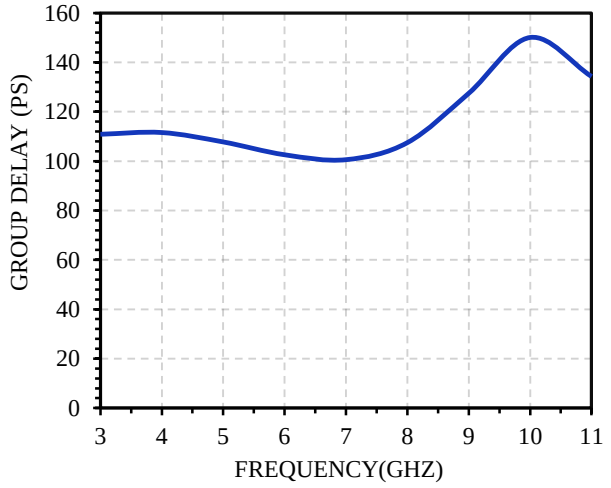

Fig. 6 Group delay of the proposed LNA

Based on the datasheet provided in [20], a GD variation between 100 and 150 ps is acceptable for a UWB system. Research in [18] focuses on the development of planar LNA specifically for breast cancer detection systems. The research achieved a GD variation of 103 ps, and it explained that the achieved GD is reliable and suitable for tumour detection. The research also explained that a large fluctuation in group delay can lead to pulse distortions that complicate measurement or compromise signal integrity, affecting 2D and 3D images.

Research in [19] focuses on the formation of microwave imaging for breast tumor detection. It achieved a GD range from 200 to 250 ps with a variation of 25 ps. The research explained that the achieved result is flat within the bandwidth, and the results suggest a low distortion in the system. Research in [21-23] achieved low group delay but suffered from low gain, while others [24, 25] exhibited high gain with increased group delay, highlighting the intricate design trade-offs. Maintaining these parameters is challenging due to the intricate circuit interactions.

Figure 7 shows the NF of the proposed LNA, with a minimum value of 5.2 dB. The value is higher than some reported UWB LNAs due to the design made to achieve low group delay variation while preserving a balance of gain and linearity. This is the outcome of explicit trade-offs made to maintain low group delay variation while preserving the total time-domain signal integrity.

According to [26], a UWB LNA designed for medical applications has a high NF, indicating that a relatively high NF does not always negatively impact performance. The work in [27] reports a minimum NF of 5.5 dB with comparable technology nodes, which is related to deliberate design trade-offs for wideband and integrated operation. In addition, for the same application, a study in [28] achieved a minimum NF of 6.3 dB. In conclusion, the achieved NF in the proposed design is considered an acceptable range for breast imaging systems based on the observation from the given articles. This is the outcome of intentional design to optimize gain, group delay, input matching, and linearity, which are important factors for medical imaging accuracy.

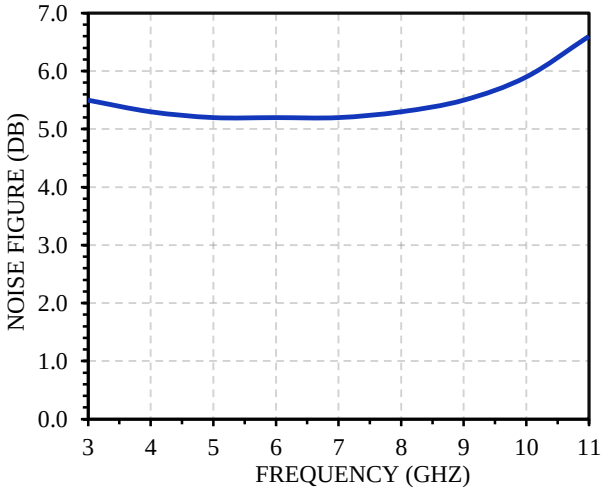

Fig. 7 Noise figure of the proposed LNA

Table 2. Comparison of the performances

Ref. & Year	CMOS Tech (nm)	Frequency (GHz)	S_{11} (dB)	S_{12} (dB)	S_{21} (dB)	GD variations (ps)	NF (dB)	IIP3 (dBm)	Area (mm^2)
This work	**180**	**3.1 – 10.6**	**<-10**	**<–33.5**	**11.2**	**±24.8**	**<6.3**	**2**	**1.24**
[24], 2018	90	3–11	<-9	<-48	20.10	±115	<5	-4.2	-
[10], 2020	90	2–30	<-15	<-95	8.7	-	19.3-5.6	4.3	-
[29], 2021	180	3.1–10.6	<-9.4	-	15.02	≈±50	<4.4	-6	1.02
[11], 2021	180	21–27	<-10.6	-	20	±58	<3.7	-8	0.49
[30], 2021	180	3.1 – 10.6	<-10	-	10.8	-	<4	2.52-7.27	0.99
[12], 2022	90	3.1 – 10.6	<-9.3	-	18.22	± 25.2	<4.68	-22.8	-
[13], 2023	180	3.1–10.6	<-10	<-25	11	-	<4.3	3.95-11.65	-

Linearity is assessed through the third-order Intercept Point (IP3) and 1-dB compression points (P1dB) [12]. Based on Figure 8, the measured input P1dB is -12 dBm with an output P1dB of -1 dBm. The measurement setup has been set to a frequency spacing of 10 MHz and is centered at 6.0 GHz. The input power was swept from -26 to 4 dBm, with the fundamental and third-order signal responses projected. The suggested design's IIP3 measured 2 dBm, with an output Third-Order Intercept Point (OIP3) of 14 dBm.

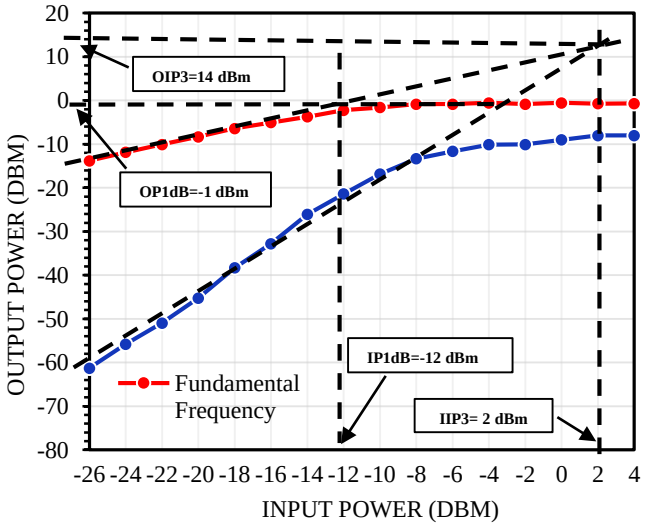

Fig. 8 Measured 1-dB compression point (P1dB) and third-order intercept point (IIP3)

Table 2 shows a comparison of this work to existing work. Table 2 demonstrates that the proposed UWB LNA achieves one of the lowest GD variations among the reported works, with only ±24.8 ps across the 3.1-10.6 GHz band. This work is closely comparable to [12] in terms of the GD; however, it requires a more advanced CMOS 90 nm design technology. The higher group delay performance is accomplished by optimizing the inductors' configuration (Ls_2, Lg_1, Ld_3), correct input matching, and phase linearization, which decrease reflections and stabilize the phase response over the frequency band.

In addition, maintaining a flat GD ensures minimal pulse distortion, preserving signal integrity, which is especially important for applications such as UWB imaging and breast tumor detection. In addition, despite its good GD performance, the design has a major limitation in linearity, with an IIP3 of −22.8 dBm, which is significantly poorer than most works in the table.

Additionally, the suggested design achieves a respectable average measured gain of 11.2 dB. In addition, this research shows exceptional linearity, reaching a maximum IIP3 of 2 dBm. Due to less research on UWB LNA specifically focusing on group delay variation from recent years, direct comparison is limited. Research in [13, 30] did not include group delay variation as one of their parameters; hence, comparisons are made on other performance parameters.

5. Conclusion

A 3.1 to 10.6 GHz LNA is presented for breast imaging applications using a 180 nm CMOS process. The novelty of this work lies in a hybrid LNA configuration that combines a cascoded topology with inductive source degeneration and inductive peaking, providing that careful inductor selection and tuning may successfully control phase linearity and group delay variation.

This design prioritizes low group delay distortion as a main performance parameter for maintaining time-domain signal integrity in breast imaging applications. It also aims to achieve high gain and low delay distortion for breast imaging systems. The measurement results demonstrate that the LNA has an average gain of 11.2 dB, a minimum NF of 5.2 dB, and input matching of less than –10 dB. The proposed design achieved an IIP3 of 2 dBm at a 6 GHz center frequency with 10 MHz spacing. It also exhibits a group delay of ± 24.8 ps

and a chip area of 1.24 mm², including the I/O pad. The proposed design achieves improved group delay flatness through the optimized use of inductive elements in the LNA. The source degeneration and gate inductors enable broadband input matching and improved phase linearity, while the inductive peaking at the drain helps to flatten the phase response at higher frequencies. The proposed design demonstrates that careful inductor optimization can effectively reduce group delay variation while maintaining acceptable gain, linearity, and noise performance. Moreover, the theoretical analysis determines that low base inductance was beneficial to achieve minimum group delay variation while maintaining other parameters.

Funding Statement

The author would like to thank the Ministry of Higher Education, Malaysia, Fundamental Research Grant Scheme (FRGS/1/2020/TK0/UNIMAS/02/6), and Universiti Malaysia Sarawak (F02/FRGS/2005/2020) for the funding to support this research work.

Acknowledgments

The author would like to thank the Collaborative micro-Electronic Design Excellence Centre (CEDEC) and the Sponsorship Section, Ministry of Higher Education, Malaysia, for supporting this work.

References

[1] Essex J. Bond et al., "Microwave Imaging via Space-Time Beamforming for Early Detection of Breast Cancer," *IEEE Transactions on Antennas and Propagation*, vol. 51, no. 8, pp. 1690-1705, 2003. [CrossRef] [Google Scholar] [Publisher Link]

[2] Sunjoo Hong et al., "A 4.9 mΩ-Sensitivity Mobile Electrical Impedance Tomography IC for Early Breast-Cancer Detection System," *IEEE Journal of Solid-State Circuits*, vol. 50, no. 1, pp. 245-257, 2015. [CrossRef] [Google Scholar] [Publisher Link]

[3] Sarmad Maqsood, Robertas Damaševičius, and Rytis Maskeliūnas, "TTCNN: A Breast Cancer Detection and Classification towards Computer-Aided Diagnosis using Digital Mammography in Early Stages," *Applied Sciences*, vol. 12, no. 7, pp. 1-27, 2022. [CrossRef] [Google Scholar] [Publisher Link]

[4] Gelan Ayana, Kokeb Dese, and Se-woon Choe, "Transfer Learning in Breast Cancer Diagnoses via Ultrasound Imaging," *Cancers*, vol. 13, no. 4, pp. 1-15, 2021. [CrossRef] [Google Scholar] [Publisher Link]

[5] Maged A. Aldhaeebi et al., "Review of Microwave Techniques for Breast Cancer Detection," *Sensors*, vol. 20, no. 8, pp. 1-38, 2020. [CrossRef] [Google Scholar] [Publisher Link]

[6] Nour AlSawaftah et al., "Microwave Imaging for Early Breast Cancer Detection: Current State, Challenges, and Future Directions," *Journal of Imaging*, vol. 8, no. 5, pp. 1-31, 2022. [CrossRef] [Google Scholar] [Publisher Link]

[7] Xiaolu Guo et al., "Simulation and Design of a UWB Imaging System for Breast Cancer Detection," *Integration*, vol. 47, no. 4, pp. 548-559, 2014. [CrossRef] [Google Scholar] [Publisher Link]

[8] Francesco Colonna et al., "Hardware Acceleration of Beamforming in a UWB Imaging Unit for Breast Cancer Detection," *VLSI Design*, vol. 2013, pp. 1-11, 2013. [CrossRef] [Google Scholar] [Publisher Link]

[9] Shahab Shahrabadi, "Ultrawideband LNA 1960-2019: Review," *IET Circuits, Devices & Systems*, vol. 15, no. 8, pp. 697-727, 2021. [CrossRef] [Google Scholar] [Publisher Link]

[10] Deepak Prasad et al., "A Novel Design of UWB Low Noise Amplifier for 2-10 GHz Wireless Sensor Applications," *Sensors International*, vol. 1, pp. 1-6, 2020. [CrossRef] [Google Scholar] [Publisher Link]

[11] Vikram Singh, Sandeep Kumar Arya, and Manoj Kumar, "A Common-Gate Current-Reuse UWB LNA for Wireless Applications in 90 nm CMOS," *Wireless Personal Communications*, vol. 119, no. 2, pp. 1405-1423, 2021. [CrossRef] [Google Scholar] [Publisher Link]

[12] Humirah Majeed, and Vikram Singh, "A Common-Gate, gm-Boosting LNA using Active Inductor-Based Input Matching for 3.1-10.6 GHz UWB Applications," *Electrica*, vol. 22, no. 2, pp. 173-187, 2022. [CrossRef] [Google Scholar] [Publisher Link]

[13] B. Dorostkar Yaghouti, "A Novel High-Linearity LNA based on Post Distortion and CDS Techniques for UWB Radar," *Iranian Journal of Electrical and Electronic Engineering*, vol. 19, no. 2, pp. 279-290, 2023. [Google Scholar]

[14] Vikram Singh, Manoj Kumar, and Nitin Kumar, "Design of a Low Power LNA Circuit with Noise Canceling Approach in 90 nm CMOS Process," *Integration*, vol. 96, 2024. [CrossRef] [Google Scholar] [Publisher Link]

[15] Xiyang Wang, Tao Men, and Buwen Cheng, "A 6-18 GHz Low-Noise Amplifier with 19 dBm OP1dB and 2.6 ± 0.3 dB NF in 0.15 μm GaAs Process," *Electronics*, vol. 14, no. 8, pp. 1-12, 2025. [CrossRef] [Google Scholar] [Publisher Link]

[16] Bofan Chen et al., "Ultra-Wideband High-Gain Low Group Delay Variation Amplifier for Phased-Array Radar System," *Microelectronics Journal*, vol. 146, 2024. [CrossRef] [Google Scholar] [Publisher Link]

[17] Umair Rafique et al., "Ultra-Wideband Antennas for Biomedical Imaging Applications: A Survey," *Sensors*, vol. 22, no. 9, pp. 1-38, 2022. [CrossRef] [Google Scholar] [Publisher Link]

[18] Moustapha El Bakkali et al., "Improving Sensitivity and Selectivity of Breast Cancer Detection Systems through the Development of a High-Performance LNA," *2024 6th International Symposium on Advanced Electrical and Communication Technologies (ISAECT)*, Alkhobar, Saudi Arabia, pp. 1-6, 2024. [CrossRef] [Google Scholar] [Publisher Link]

[19] Carolina Blanco-Angulo et al., "Non-Invasive Microwave-Based Imaging System for Early Detection of Breast Tumours," *Biosensors*, vol. 12, no. 9, pp. 1-24, 2022. [CrossRef] [Google Scholar] [Publisher Link]

[20] AccuraUWB FXUWB01 Datasheet, Accura Technologies, 2020. [Online]. Available: https://www.taoglas.com/datasheets/FXUWB01.07.0100C.pdf

[21] Jen-How Lee et al., "A 2.5-dB NF 3.1-10.6-GHz CMOS UWB LNA with Small Group-Delay-Variation," *2008 IEEE Radio Frequency Integrated Circuits Symposium*, Atlanta, GA, pp. 501-504, 2008. [CrossRef] [Google Scholar] [Publisher Link]

[22] Chi-Chen Chen, Hung-Yu Yang, and Yo-Sheng Lin, "A 21-27 GHz CMOS Wideband LNA with 9.3 ± 1.3 dB Gain and 103.9 ± 8.1 ps Group-Delay using Standard 0.18 μm CMOS Technology," *2009 IEEE Radio and Wireless Symposium*, San Diego, CA, USA, pp. 586-589, 2009. [CrossRef] [Google Scholar] [Publisher Link]

[23] Reza Erfani, Fatemeh Marefat, and Mehdi Ehsanian, "Highly Phase-Linear Self-Biased CMOS IR-UWB LNA with Sub-ps Group-Delay Variations," *2016 28th International Conference on Microelectronics (ICM)*, Giza, Egypt, pp. 153-156, 2016. [CrossRef] [Google Scholar] [Publisher Link]

[24] Sunil Pandey, Tushar Gawande, and Pravin N. Kondekar, "A 3.1-10.6 GHz UWB LNA based on Self-Cascode Technique for Improved Bandwidth and High Gain," *Wireless Personal Communications*, vol. 101, no. 3, pp. 1867-1882, 2018. [CrossRef] [Google Scholar] [Publisher Link]

[25] Sunil Pandey, Tushar Gawande, and Pravin N. Kondekar, "A 0.9 V, 4.57 mW UWB LNA with Improved Gain and Low Power Consumption for 3.1-10.6 GHz Ultra-Wideband Applications," *Wireless Personal Communications*, vol. 96, no. 4, pp. 583-597, 2017. [CrossRef] [Google Scholar] [Publisher Link]

[26] Abolfazl Bijari, Fereshte Khoshbinahmadi, and Mohammad-Amin Mallaki "An Ultra-Low-Power Low-Noise Amplifier using Current Reuse and Self-Forward Body Bias Techniques for Biomedical Applications," *International Journal of Circuit Theory and Applications*, vol. 53, no. 2, pp. 571-594, 2024. [CrossRef] [Google Scholar] [Publisher Link]

[27] Atakan Aydoğdu et al., "A 2.55-mW On-Chip Passive Balun-LNA in 180-nm CMOS," *Analog Integrated Circuits and Signal Processing*, vol. 111, no. 2, pp. 223-234, 2022. [CrossRef] [Google Scholar] [Publisher Link]

[28] Leonardo Rodrigues Leopoldo, and Wilhelmus A.M. Van Noije, "Low Noise Broadband Amplifier for Breast Cancer System," *2022 35th SBC/SBMicro/IEEE/ACM Symposium on Integrated Circuits and Systems Design (SBCCI)*, Porto Alegre, Brazil, pp. 1-5, 2022. [CrossRef] [Google Scholar] [Publisher Link]

[29] To-Po Wang, "Design and Analysis of Simultaneous Wideband Input/Output Matching Technique for Ultra-Wideband Amplifier," *IEEE Access*, vol. 9, pp. 46800-46809, 2021. [CrossRef] [Google Scholar] [Publisher Link]

[30] Behnam Dorostkar Yaghouti, and Javad Yavandhasani, "A High Linearity Low Power Low-Noise Amplifier Designed for Ultra-Wide-Band Receivers," *Analog Integrated Circuits and Signal Processing*, vol. 107, no. 1, pp. 109-120, 2021. [CrossRef] [Google Scholar] [Publisher Link]